

Research Article

Axisymmetric Free Vibration Analysis of Annular and Circular Mindlin Plates Using the Nonlocal Continuum Theory

Ma'en S. Sari

Department of Mechanical Engineering, King Faisal University, Al-Hasa, Saudi Arabia

Abstract: This study aims to investigate and analyze the axisymmetric free vibration of non-local annular and circular Mindlin plates at the micro/nano scale which are modeled using Eringen's nonlocal elasticity theory, taking into consideration the small scale effect. The governing equations are derived using the nonlocal differential constitutive relations of Eringen. For this purpose, the resulted eigenvalue problem is solved numerically by applying the Chebyshev collocation method. The effects of the inner to outer radius ratio, the thickness to outer radius ratio, the nonlocal scale effect and the boundary conditions on the natural frequencies are studied.

Keywords: Annular and circular mindlin plates, axisymmetric vibration, chebyshev collocation method, eigenvalue problem, eringen's non-local elasticity theory, natural frequencies

INTRODUCTION

Due to their significant role in different engineering and modern technology fields such as aerospace, communications, composites, electronics, micro electro mechanical systems and nano electromechanical systems, micro and nano structures have gained appreciated consideration. These structures have more superior mechanical, electrical and thermal properties comparing with other structures at the normal length scale as they are high sensitive and high frequency devices for different applications (Murmu and Pardhan, 2009a).

In order to design a realistic model of a micro or a nanostructure, optimize and improve their performance and to well understand it, the small-scale effects and the atomic forces must be taken into consideration. In objects at the micro and nano scales, the dimensions, wavelengths and sizes of these structures are no longer considered much larger than the characteristic dimensions of the microstructure. In these cases, the internal length scales of the material are comparable with the structure size. Moreover, the particles affect each other by long range cohesive forces in addition to the contact forces and heat diffusion. Consequently, the internal length scale should be considered as a material parameter called nonlocal parameter in the constitutive and governing equations and relations.

Although the experimental and atomistic simulations and models are both capable to show the effects of the small-scale on the mechanical properties of the micro/nanostructures, these methods are expensive and restricted by computational capacity. It is well known that the local continuum theories for beams (Euler and Timoshenko) and plates (Kirchhoff and

Mindlin) are scale free. Therefore, they are not able to capture the small scale effect on the mechanical, electrical and thermal properties for very small beam and plate like structures, which makes them inadequate in describing the dynamical behavior for these structures (Wang *et al.*, 2007). In order to apply the continuum mechanics approach in the analysis of the micro and nanostructures, logical and reasonable modifications that take into consideration the scale effect should be proposed. For this purpose, several theoretical models have been suggested, such as the strain gradient theory, the modified coupled stress theory and the nonlocal elasticity theory which will be utilized in this study to analyze the free vibration problem of nonlocal annular and circular Mindlin plates.

The nonlocal elasticity theory was introduced by Eringen (1983) accounts for the small-scale effects arising at the nano scale level by assuming that the stress at a point is a function of the strains at all points in the domain. Many researchers applied the nonlocal elasticity theory to study the free vibration, buckling, deflection and dynamic problems of micro and nanostructures. For example, Reddy (2007) obtained analytical solutions for the bending, buckling and vibration problems for simply supported Euler, Timoshenko, Reddy and Levinson beams using Eringen's nonlocal theory. Murmu and Adhikari (2010a) studied the nonlocal transverse in and out-of-phase vibrations of double nanobeam systems, in which explicit closed-form expressions for natural frequencies were derived.

Shakouri *et al.* (2011) applied the Galerkin approach to study the free vibration problem of nonlocal Kirchhoff plates with different boundary

conditions; this study showed that the nonlocal parameter and Poisson's ratio have significant effects on the vibration. Wang *et al.* (2007) applied the Hamilton's principle, Eringen's nonlocal elasticity theory and Timoshenko beam theory to analyze the free vibration problem of the micro/nanobeams; it was concluded that the effects of small scale, rotary inertia and transverse shear deformation are important on the vibration behavior of short, stubby micro/nanobeams. Moreover, Murmu and Adhikari (2010b) applied the differential quadrature method and the nonlocal elasticity theory to study the free vibration of a rotating carbon nanotube modeled as an Euler-Bernoulli beam. It was concluded that the vibration is significantly influenced by the angular velocity, preload and the nonlocal parameter.

Lu *et al.* (2006) derived the dispersion relation for a harmonic flexural wave propagation in an Euler-Bernoulli beam, as well as the frequency equations and modal shape functions for beam with different boundary conditions based on Eringen's nonlocal elasticity theory. Murmu and Pradhan (2009b) implemented the nonlocal elasticity theory to study the vibration response of single graphene sheets embedded in an elastic medium modeled as Winkler and Pasternak foundations, where the differential quadrature method was employed to numerically solve for the fundamental natural frequencies of plates with clamped and simply supported edges. In a similar manner, Murmu and Pradhan (2009b) applied the nonlocal elasticity theory to investigate the free vibration problem of nanoplates under uniaxially pre stressed conditions by utilizing the differential quadrature method to obtain the fundamental natural frequencies for simply supported and clamped nanoplates. In this study, it was observed that buckling occurs at smaller critical compressive load compared to the classical plate theory.

Gürses *et al.* (2012) studied the free vibration analysis of thin nano-sized annular sector plates utilizing Eringen's nonlocal elasticity theory to formulate the equation of motion. The discrete singular convolution method was applied after transforming the irregular physical domain into a rectangular domain by using geometric coordinate transformation. This study showed that the effects of the nonlocal parameter is significant in the vibration analysis. Hashemi *et al.* (2013a) applied an exact analytical approach along with Eringen's theory to study the free vibration problem of thick circular and annular functionally graded Mindlin nanoplates with different combinations of boundary conditions. The effects of the plate radius, material properties which vary through the material according to a power-law distribution and the nonlocal parameter on the natural frequencies were examined. In another study, Hashemi *et al.* (2013b) introduced potential functions and used the separation of variables method to obtain closed-form solutions for non-local rectangular Mindlin plates with Levy-type boundary

conditions in which the effects of the nonlocal parameter, thickness to length ratio and aspect ratio on the natural frequencies were investigated.

Furthermore, Ansari *et al.* (2010) applied the generalized differential quadrature method, Eringen's nonlocal elasticity theory and the molecular dynamics simulations to carry out the vibration analysis of single layered graphene sheets modeled as rectangular Mindlin plates. Additionally, the appropriate values of the nonlocal parameter suitable for each boundary condition were evaluated. Duan and Wang (2007) obtained exact solutions for the axisymmetric bending of micro and nano circular plates under general loading using a nonlocal plate theory. It was concluded that nonlocal parameter has a significant effect on the deflections, moments and bending stiffness.

The main objective of this article is to study the axisymmetric free vibration problem of non-local annular and circular Mindlin plates. For this purpose, Eringen's nonlocal elasticity theory along with Hamilton's principle will be applied and the Chebyshev collocation method (as a numerical technique) will be used to discretize the problem and to obtain the algebraic eigenvalue problem and hence, solving for the natural frequencies. It is worthwhile to mention that the Chebyshev collocation method was successfully employed to carry out the free vibration analysis of local continuous systems with different shapes and geometries in previous studies (Sari *et al.*, 2011; Sari and Butcher, 2011a, b, 2012).

MATERIALS AND METHODS

Chebyshev spectral collocation: Gauss-Chebyshev-Lobatto or Chebyshev extreme points are the points in the interval $(-1, 1)$ defined by:

$$x_j = \cos(j\pi/N), \quad j = 0, 1, \dots, N \quad (1)$$

Chebyshev points are the projections on $(-1, 1)$ of equally spaced points on the upper half of the unit circle and they are numbered from right to left as shown in Fig. 1 (Trefethen, 2000). For the set of $N+1$ Chebyshev points we have an $(N+1) \times (N+1)$ Chebyshev differentiation matrix D_N . The Chebyshev differentiation matrix is obtained by interpolating a Lagrange polynomial of degree N at each Chebyshev point, differentiating the polynomial and then finding the derivative of the polynomial at each Chebyshev point. The entries of this matrix are:

$$(D_N)_{00} = \frac{2N^2+1}{6}, (D_N)_{NN} = -\frac{2N^2+1}{6}, (D_N)_{jj} = \frac{-x_j}{2(1-x_j^2)}, \quad (2)$$

$$j = 1, \dots, N-1 (D_N)_{jj} = \frac{c_i (-1)^{i+j}}{c_j (x_i - x_j)},$$

$$i \neq j, \quad i, j = 0, \dots, N. \quad c_i = \begin{cases} 2, & i = 0 \text{ or } N, \\ 1, & \text{otherwise} \end{cases}$$

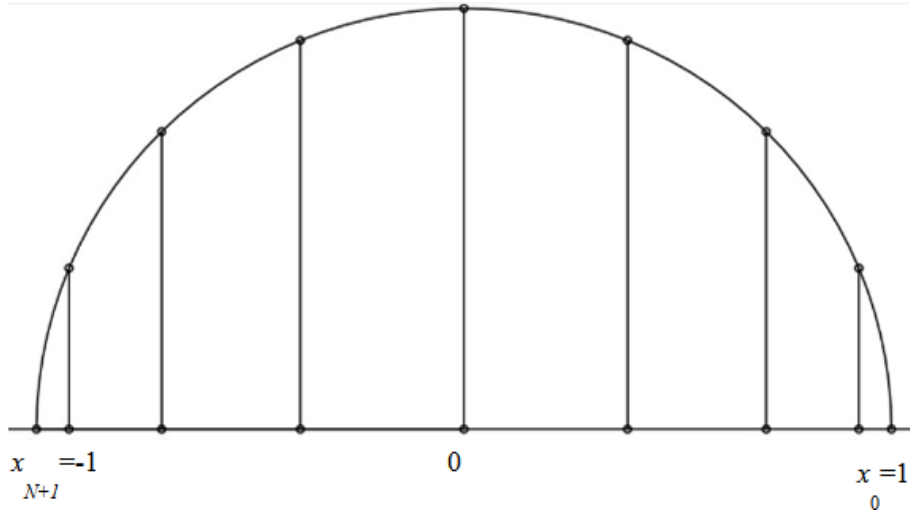


Fig. 1: Chebyshev points

When solving ODEs or PDEs by the Chebyshev collocation method, the first derivative is represented by $D1 = D_N$, the second derivative by $D2 = (D1)^2 = (D_N)^2$ and so on.

Nonlocal theory: In local elasticity theory, the stress at a reference point in a body depends on the strain at the same point. On the other hand, In the non-local elasticity theory pioneered by Eringen (1983), the stress at a point in a linear, homogeneous, isotropic, elastic domain is related to the stress field at all points in the domain. Eringen's theory is based on the atomic theory of lattice dynamics and experimental results on phonon scattering and dispersion (Eringen, 1983; Gürses *et al.*, 2012). For non-local linear elastic solids, the stress tensor t_{ij} is defined by:

$$t_{ij} = \int_V \alpha(|x' - x|) \sigma_{ij}(x') dV(x') \quad (3)$$

where, x is a reference point in the elastic domain, $\alpha(|x' - x|)$ is the non-local kernel attenuation function which introduces the nonlocal effects at the reference point x produced by the local stress σ_{ij} at any point x' and $|x' - x|$ is the distance in Euclidean form.

In order to simplify Eq. (1), Eringen introduced a linear differential operator ζ , defined by $\zeta = 1 - (e_0 l)^2 \nabla^2$ in which e_0 is a material constant estimated by experiments or other models and theories, such that the non-local theory relations could result in approximate solutions to those obtained by atomic theory. The value of e_0 was taken to be 0.39 in Eringen's analysis. Moreover, the constant l represents the internal characteristic length which is of the same order of the external length. The Laplace operator ∇^2 is defined in the polar coordinates as:

$$\nabla^2 = \frac{\partial^2}{\partial r^2} + \frac{1}{r} \frac{\partial}{\partial r} + \frac{\partial^2}{\partial \theta^2}$$

Since the axisymmetric vibration of the annular non-local Mindlin plates will be studied, all derivatives with respect to the θ axis will be zero and hence, the Laplace operator is simplified as:

$$\nabla^2 = \frac{\partial^2}{\partial r^2} + \frac{1}{r} \frac{\partial}{\partial r} \quad (4)$$

According to Eringen, the integral constitutive relation Eq. (1) could be simplified and rewritten as:

$$\left(1 - (e_0 l)^2 \nabla^2\right) t_{ij} = \sigma_{ij} \quad (5)$$

Due to its simple form, Eq. (3) has been extensively employed by many researchers in applying the non-local theory to study and analyze the vibration and mechanics of micro and nanostructures.

From Eq. (3) and utilizing Hook's law, the constitutive relations can be expressed as:

$$\sigma_r - (e_0 l)^2 \left(\frac{\partial^2 \sigma_r}{\partial r^2} + \frac{1}{r} \frac{\partial \sigma_r}{\partial r} \right) = \frac{E}{1 - \nu^2} (\varepsilon_r + \nu \varepsilon_\theta), \quad (6)$$

$$\sigma_\theta - (e_0 l)^2 \left(\frac{\partial^2 \sigma_\theta}{\partial r^2} + \frac{1}{r} \frac{\partial \sigma_\theta}{\partial r} \right) = \frac{E}{1 - \nu^2} (\varepsilon_\theta + \nu \varepsilon_r), \quad (7)$$

where,

- σ_r and ε_r : The normal stress and normal strain in the radial direction r
- σ_θ and ε_θ : The normal stress and normal strain in the circumferential direction θ

E : Young's modulus
 ν : The Poisson's ratio

In the case of axisymmetric vibration, the normal strains ϵ_r and ϵ_θ are defined as:

$$\epsilon_r = z \frac{\partial \psi}{\partial r}, \quad \epsilon_\theta = z \frac{\psi}{r} \quad (8)$$

where, the z axis is shown in Fig. 2 and ψ is the slope rotation in the r - z plane at $z = 0$.

Accordingly, the resultant moments and shear are expressed as:

$$M_r - (e_0 a)^2 \left(\frac{\partial^2 M_r}{\partial r^2} + \frac{1}{r} \frac{\partial M_r}{\partial r} \right) = D \left(\frac{\partial \psi}{\partial r} + \nu \frac{\psi}{r} \right) \quad (9)$$

$$M_\theta - (e_0 a)^2 \left(\frac{\partial^2 M_\theta}{\partial r^2} + \frac{1}{r} \frac{\partial M_\theta}{\partial r} \right) = D \left(\nu \frac{\partial \psi}{\partial r} + \frac{\psi}{r} \right) \quad (10)$$

$$Q_r - (e_0 a)^2 \left(\frac{\partial^2 Q_r}{\partial r^2} + \frac{1}{r} \frac{\partial Q_r}{\partial r} \right) = \kappa G h \left(\frac{\partial w}{\partial r} + \psi \right) \quad (11)$$

where,
 $\bar{w}(r, t)$: The transverse deflection
 $D = Eh^3/12(1-\nu^2)$: The flexural rigidity

h : The thickness
 κ : The shear correction factor
 G : The shear modulus

The resultant moments and shear are defined in terms of the normal stresses σ_r and σ_θ as:

$$M_r = \int_{-h/2}^{h/2} \sigma_r z dz, \quad M_\theta = \int_{-h/2}^{h/2} \sigma_\theta z dz, \quad Q_r = \int_{-h/2}^{h/2} \sigma_r dz \quad (12)$$

Based on Hamilton's principle, the first order shear deformation theory FSDT and Eringen's non-local constitutive relations, the following equilibrium equations of the free vibration are obtained for an annular axisymmetric isotropic non-local Mindlin plate with a uniform thickness shown in Fig. 2:

$$\begin{aligned} \frac{\partial M_r}{\partial r} + \frac{M_r - M_\theta}{r} - Q_r &= (1 - (e_0 l)^2 \nabla^2) \frac{\rho h^3}{12} \frac{\partial^2 \bar{w}}{\partial t^2} \\ \frac{\partial Q_r}{\partial r} + \frac{Q_r}{r} &= (1 - (e_0 l)^2 \nabla^2) \rho h \frac{\partial^2 \bar{w}}{\partial t^2} \end{aligned} \quad (13)$$

where,
 t = The time
 ρ = The density of plate material

Substituting Eq. (9)-(12) into Eq. (13) yields:

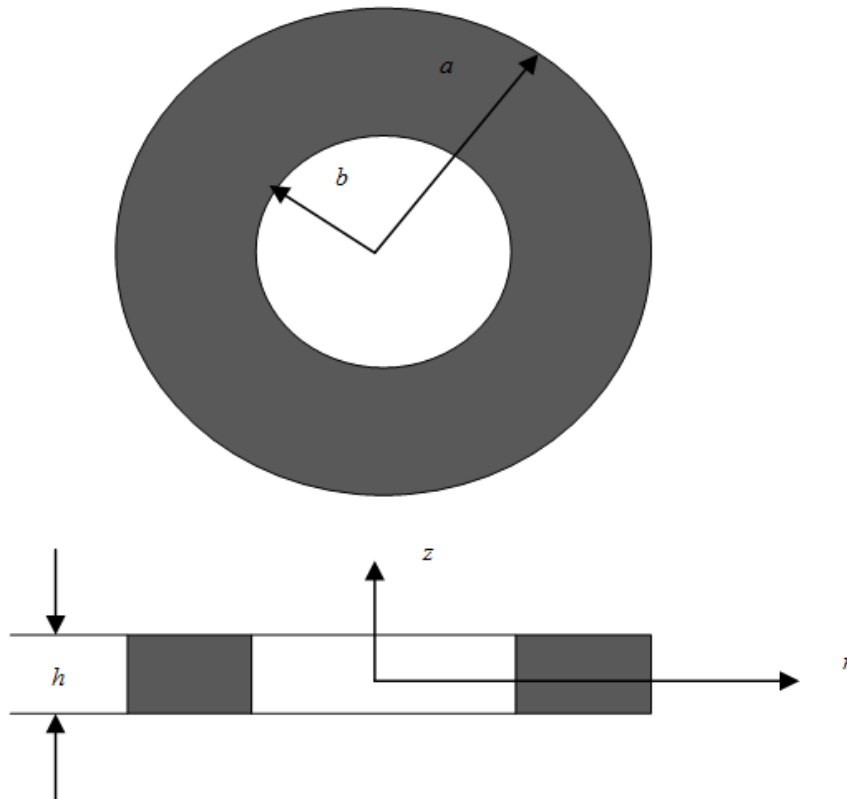


Fig. 2: The thick annular plate under consideration

$$\begin{aligned}
 D \left(\frac{\partial^2 \bar{\psi}}{\partial r^2} + \frac{1}{r} \frac{\partial \bar{\psi}}{\partial r} - \frac{\bar{\psi}}{r^2} \right) - \kappa Gh \left(\frac{\partial \bar{w}}{\partial r} + \bar{\psi} \right) &= \frac{\rho h^3}{12} \left(\frac{\partial^2 \bar{\psi}}{\partial t^2} - (e_0 l)^2 \frac{\partial^4 \bar{\psi}}{\partial t^2 \partial r^2} - \frac{(e_0 l)^2}{r} \frac{\partial^3 \bar{\psi}}{\partial t^2 \partial r} \right) \\
 \kappa Gh \left(\frac{\partial^2 \bar{w}}{\partial r^2} + \frac{1}{r} \frac{\partial \bar{w}}{\partial r} + \frac{\partial \bar{\psi}}{\partial r} + \frac{\bar{\psi}}{r} \right) &= \rho h \left(\frac{\partial^2 \bar{w}}{\partial t^2} - (e_0 l)^2 \frac{\partial^4 \bar{w}}{\partial t^2 \partial r^2} - \frac{(e_0 l)^2}{r} \frac{\partial^3 \bar{w}}{\partial t^2 \partial r} \right)
 \end{aligned} \tag{14}$$

Note that the governing Eq. (14) reduce to that of the local Annular Mindlin plate model when the characteristic length l is set to zero (Han and Liew, 1999).

For convenience, the following non-dimensional parameters are introduced:

$$R = \frac{r}{a}, \quad \delta = \frac{h}{a}, \quad \beta = \frac{b}{a}, \quad W = \frac{\bar{w}}{a}, \quad \Psi = \bar{\psi}, \quad T = t \left(\frac{E}{\rho a^2 (1-\nu^2)} \right)^{1/2}, \quad \mu = \frac{e_0 l}{a}$$

And assuming harmonic solutions in time as:

$$\bar{\psi}(R, T) = \psi(R) e^{i\Omega T}, \quad \bar{w}(R, T) = w(R) e^{i\Omega T} \tag{15}$$

Yields:

$$\begin{aligned}
 \delta^2 \left(R^2 \frac{d^2 \Psi}{dR^2} + R \frac{d\Psi}{dR} - \Psi \right) - 6\kappa(1-\nu)R^2 \left(\frac{dW}{dR} + \Psi \right) &= -\delta^2 R^2 \Omega^2 \Psi + \mu^2 \delta^2 R^2 \Omega^2 \frac{d^2 \Psi}{dR^2} \\
 &\quad + \mu^2 \delta^2 R \Omega^2 \frac{d\Psi}{dR} \\
 R \frac{d^2 W}{dR^2} + \frac{dW}{dR} + R \frac{d\Psi}{dR} + \Psi &= -\frac{2R\Omega^2}{(1-\nu)\kappa} W + \frac{2\mu^2 R\Omega^2}{(1-\nu)\kappa} \frac{d^2 W}{dR^2} + \frac{2\mu^2 \Omega^2}{(1-\nu)\kappa} \frac{dW}{dR}
 \end{aligned} \tag{16}$$

The left hand side of each equation is written in terms of Chebyshev collocation matrices and the Kronecker product operator as:

$$\begin{aligned}
 GE1 &= [1 \ 0] \otimes \left((\delta^2 \text{diag}(R^2) * D2) + (\delta^2 \text{diag}(R) * D1) - (\delta^2 I) - (6\kappa(1-\nu) \text{diag}(R^2)) \right) + \\
 &\quad [0 \ 1] \otimes (-6\kappa(1-\nu) \text{diag}(R^2) * D1) \\
 GE2 &= [1 \ 0] \otimes ((\text{diag}(R) * D1) + (I)) + [0 \ 1] \otimes ((\text{diag}(R) * D2) + (D1))
 \end{aligned}$$

The right hand side of each equation is written as:

$$\begin{aligned}
 RH1 &= [1 \ 0] \otimes \left((-\delta^2 \text{diag}(R^2)) + (\mu^2 \delta^2 \text{diag}(R^2) D2) + (\mu^2 \delta^2 \text{diag}(R) D1) \right) \\
 RH2 &= [0 \ 1] \otimes \left(\left(-\frac{2}{(1-\nu)\kappa} \text{diag}(R) \right) + \left(\frac{2\mu^2}{(1-\nu)\kappa} \text{diag}(R) D2 \right) + \left(\frac{2\mu^2}{(1-\nu)\kappa} D1 \right) \right)
 \end{aligned}$$

where, $\text{diag}(R)$ and $\text{diag}(R^2)$ are diagonal $M \times M$ matrices with values of R_i and R_i^2 on the main diagonals, respectively and $M = N+1$ and $i = 2, 3, \dots, N$. The dimensions of $GE1$, $GE2$, $RH1$ and $RH2$ are $M \times 2M$. Equation (16) is written as:

$$\begin{bmatrix} GE1 \\ GE2 \end{bmatrix} \begin{Bmatrix} \Psi \\ W \end{Bmatrix} = \Omega^2 \begin{bmatrix} RH1 \\ RH2 \end{bmatrix} \begin{Bmatrix} \Psi \\ W \end{Bmatrix} \tag{17}$$

It is worthwhile to mention that for the annular plates, the Chebyshev points are shifted to the range $[b/a, 1]$, while for the circular plates these points are shifted to the range $[0, 1]$ as the solid part of the annulus begins at $r = b$ or $R = b/a$. This different range of the points in both cases leads to different Chebyshev differentiation matrices since the entries of these matrices depend on the distribution of the points.

Boundary conditions: In order to obtain the natural frequencies of the circular annular non-local Mindlin plate, the boundary conditions at $r = b$ and at $r = a$ should be applied. In the present study, two types of boundary conditions, i.e., simply Supported (S) and Clamped (C) are taken into consideration. For a clamped edge, both displacements W and Ψ equal zero; whereas for a simply supported edge, the transverse displacement W and M_r equal zero. In terms of Chebyshev collocation method, these conditions are applied at the inner edge ($r = b$) as:

Clamped: $W_I = 0 \Rightarrow ([0 \ 1] \otimes [1 \ \dots \ 0])(U)^T = 0$:

$$\Psi_I = 0 \Rightarrow ([1 \ 0] \otimes [1 \ \dots \ 0])(U)^T = 0 \tag{18}$$

where, $[1 \ \dots \ 0]$ is a $1 \times M$ vector with the first entry equals one and other entries are zero since it corresponds to the boundary $r = b$. The displacement vector $[U]$ is defined as:

$$[U] = \begin{Bmatrix} \Psi \\ W \end{Bmatrix}$$

Simply supported:

$$\begin{aligned} W_I = 0 &\Rightarrow ([0 \ 1] \otimes [1 \ \dots \ 0])(U)^T = 0 \\ M_r = 0 &\Rightarrow ([1 \ 0] \otimes DI(1,:)) + \frac{\nu}{\beta} * ([1 \ 0] \otimes [1 \ \dots \ 0])(U)^T = 0 \end{aligned} \tag{19}$$

At the outer edge ($r = a$), the conditions for the axisymmetric vibration are applied in a similar way as:
Clamped:

$$\begin{aligned} W_M = 0 &\Rightarrow ([0 \ 1] \otimes [0 \ \dots \ 1])(U)^T = 0 \\ \Psi_M = 0 &\Rightarrow ([1 \ 0] \otimes [0 \ \dots \ 1])(U)^T = 0 \end{aligned} \tag{20}$$

where, $[0 \ \dots \ 1]$ is a $1 \times M$ vector with the last entry equals one and other entries are zero since it corresponds to the boundary $r = a$.

Simply supported:

$$\begin{aligned} W_M = 0 &\Rightarrow ([0 \ 1] \otimes [0 \ \dots \ 1])(U)^T = 0 \\ M_r = 0 &\Rightarrow ([1 \ 0] \otimes DI(end,:)) + \nu * ([1 \ 0] \otimes [0 \ \dots \ 1])(U)^T = 0 \end{aligned} \tag{21}$$

where, $DI(1, :)$ is defined as:

$$DI(1,:) = [DI(1,1) \quad DI(1,2) \quad DI(1,3) \quad \dots \quad DI(1,M)]$$

and $DI(end, :)$ is defined as:

$$DI(end,:) = [DI(M,1) \quad DI(M,2) \quad DI(M,3) \quad \dots \quad DI(M,M)]$$

The boundary conditions considered here are the same for both local and nonlocal Mindlin plate models as the contribution of scale effect gets nullified at the ends as the displacements are zero. After applying the boundary conditions at $R = \beta$ and $R = l$, the system is written as:

$$\begin{bmatrix} [S_{BB}] & [S_{BI}] \\ [S_{IB}] & [S_{II}] \end{bmatrix} \begin{Bmatrix} \{U_B\} \\ \{U_I\} \end{Bmatrix} = \lambda^4 \begin{bmatrix} [0] & [0] \\ [0] & [Q] \end{bmatrix} \begin{Bmatrix} \{U_B\} \\ \{U_I\} \end{Bmatrix} \tag{22}$$

In this case, S_{BB} is a 4×4 matrix, S_{BI} is a $4 \times (2M-4)$ matrix, S_{IB} is a $(2M-4) \times 4$ matrix, S_{II} is a $(2M-4) \times (2M-4)$ matrix and U_I and U_B are the displacements vectors at the interior and boundary points, respectively. The frequency parameter λ is defined as:

$$\lambda^4 = \omega^2 a^4 \frac{\rho h}{D} \text{ and } \omega^2 = \Omega^2 \frac{E}{\rho a^2 (1-\nu^2)}$$

From the equations in matrix vector form, we obtain the final eigenvalue problem as in Eq. (22). Writing the coupled governing equations and the boundary conditions in matrix vector form with the use of the Kronecker product operator makes the procedure simpler in implementation.

For the case of axisymmetric vibration of circular non-local Mindlin plates, the governing equations are the same; whereas the Chebyshev points in this case are shifted to the range $[0, 1]$ unlike in the annular plate where these points are in the range $[b/a, 1]$. Furthermore, the boundary conditions at $R = 0$ are: Ψ and Q_R equal zero, while the edge $R = 1$ is considered to be either clamped or simply supported. It is worthwhile to mention that different range of the points in both cases leads to different Chebyshev differentiation matrices as the entries of these matrices depend on the distribution of the points.

RESULTS AND DISCUSSION

Dimensionless frequencies are calculated for annular and circular non-local Mindlin plates with clamped and simply supported boundary conditions, where $N = 16$ is used in the computations to attain convergence for the first six dimensionless frequencies. The convergence analysis for a SS non-local annular

plates, with $b/a = 0.3$, $h/a = 0.15$ and $\mu = 0.8$ are shown in Table 1, where the minimum number of points used in the computations is $N = 6$ and these points were increased till the results are converged up to four decimal places. For all cases considered in the present study, the shear correction factor is taken as $\kappa = \pi^2/12$ and the Poisson's ratio as $\nu = 0.3$.

The variation of the fundamental frequency parameter with the inner to outer radius b/a of a SS and CC annular Mindlin plates with $h/a = 0.1$ at different values of the dimensionless non-local parameter μ is presented in Fig. 3 and 4, respectively. It is shown that as the ratio b/a increases the frequency increases (Han and Liew, 1999). Further, it is observed that the natural frequency decreases by increasing the nonlocal parameter due to the decrease in the stiffness of the micro/nano-plate. In Eringen nonlocal elasticity theory, it may be viewed that atoms are bonded by elastic springs with finite value; while the classical local model assumes that the stiffness of springs have a value of infinity (Wang *et al.*, 2007; Gürses *et al.*, 2012). Moreover, it is noticed that as the non-local parameter μ increases, the frequency increases with a smaller rate as the ratio b/a increases. As an example, for the SS annular plates with $\mu = 0.1$, the fundamental frequency λ_1 increases from 13.1342 at $b/a = 0.1$ to 31.6491 at $b/a = 0.5$ with an increasing rate of about 141%; while for $\mu = 0.8$, the fundamental frequency λ_1 increases from 4.7564 at $b/a = 0.1$ to 7.3156 at $b/a = 0.5$ with an increasing rate of about 54%. For the CC annular plate

Table 1: Convergence analysis for SS non-local annular mindlin plate with $b/a = 0.3$, $h/a = 0.15$, $\mu = 0.8$

	N = 6	N = 8	N = 10	N = 12	N = 14	N = 16	N = 18
λ_1	5.2392	5.2377	5.2377	5.2377	5.2377	5.2377	5.2377
λ_2	8.8302	8.8412	8.8398	8.8399	8.8399	8.8399	8.8399
λ_3	10.9871	11.0063	10.9836	10.9850	10.9849	10.9849	10.9849
λ_4	13.7957	12.3790	12.3167	12.3108	12.3109	12.3109	12.3109
λ_5	15.4661	13.3532	13.2077	13.1514	13.1558	13.1553	13.1553
λ_6	37.2670	14.7550	13.8711	13.7361	13.7185	13.7184	13.7184

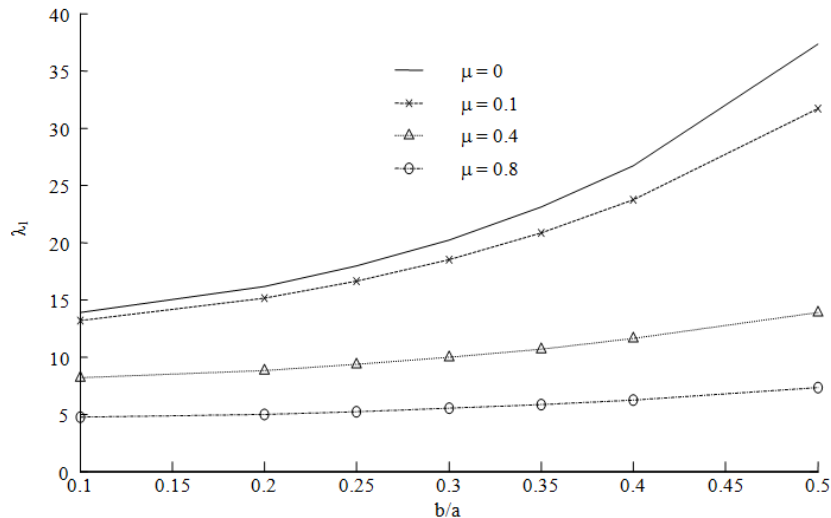


Fig. 3: Variation of the fundamental frequency parameter λ_1 with b/a of a SS non-local annular mindlin plate ($h/a = 0.1$)

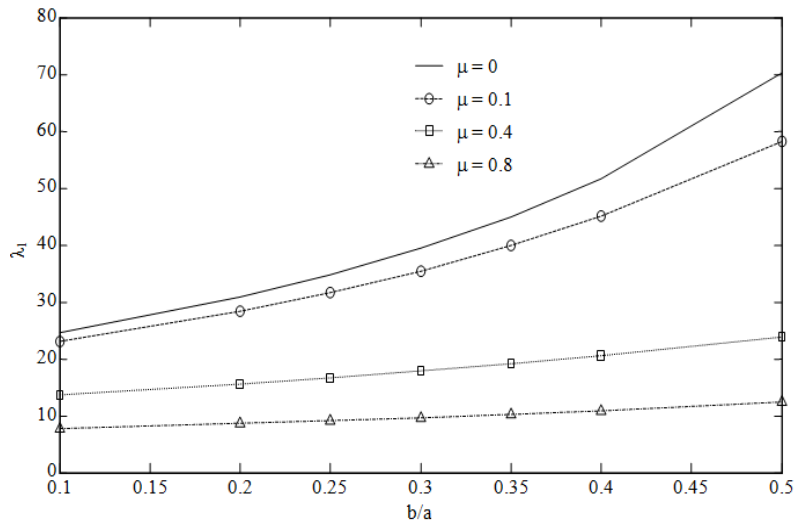


Fig. 4: Variation of the fundamental frequency parameter λ_1 with b/a of a CC non-local annular mindlin plate ($h/a = 0.1$)

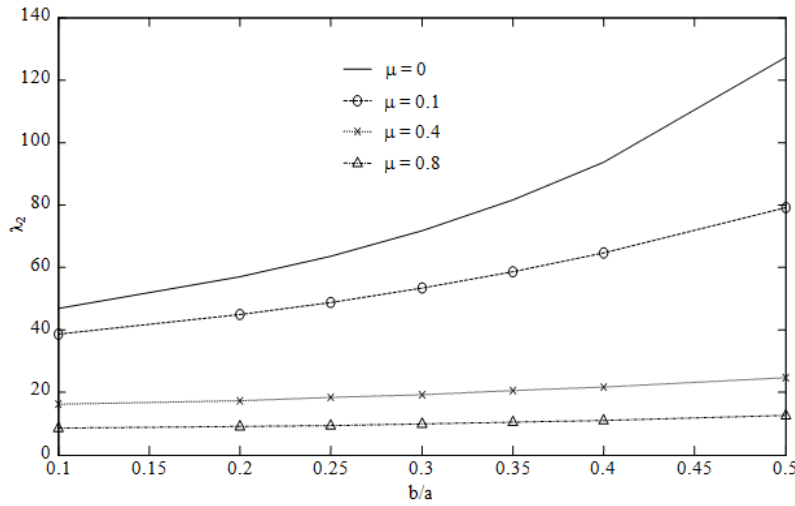


Fig. 5: Variation of the second frequency parameter λ_2 with b/a of a SS non-local annular mindlin plate ($h/a = 0.1$)

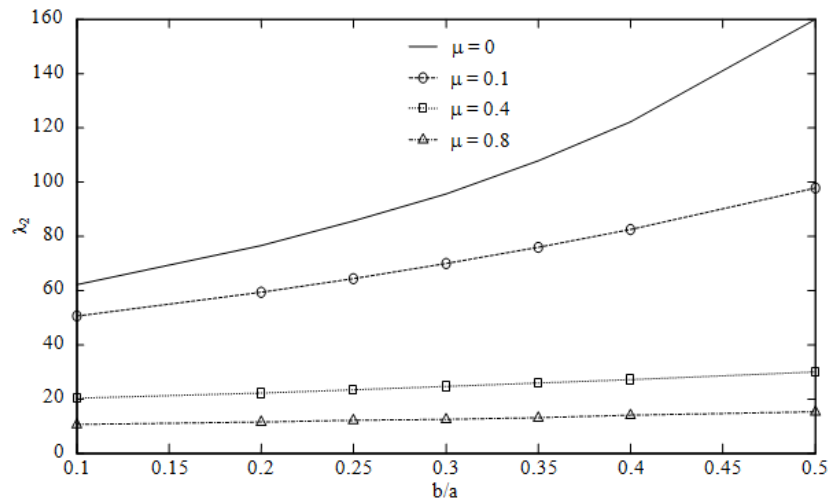


Fig. 6: Variation of the second frequency parameter λ_2 with b/a of a CC non-local annular mindlin plate ($h/a = 0.1$)

with $\mu = 0.1$, the fundamental frequency λ_1 increases from 23.1171 at $b/a = 0.1$ to 58.1934 at $b/a = 0.5$ with an increasing rate of about 152%; while for $\mu = 0.8$, the fundamental frequency λ_1 increases from 7.7659 at $b/a = 0.1$ to 12.4454 at $b/a = 0.5$ with an increasing rate of about 60%.

Similar observations may be concluded from Fig. 5 and 6 that show the variations of the second dimensionless frequencies with the inner to outer radius b/a of a SS and CC annular Mindlin plates with

$h/a = 0.1$ at different values of the dimensionless non-local parameter μ . It is seen that the second natural frequencies are more influenced by the small scale effect which can be obviously noticed from the differences between the curves for $\mu = 0$ and $\mu = 0.1$ in Fig. 3 and 5 for the SS case and between the curves for $\mu = 0$ and $\mu = 0.1$ in Fig. 4 and 6 for the CC case.

The variation of the fundamental frequency parameter with the ratio h/a of a CC non-local annular Mindlin plate with $b/a = 0.3$ is shown in Fig. 7. It is

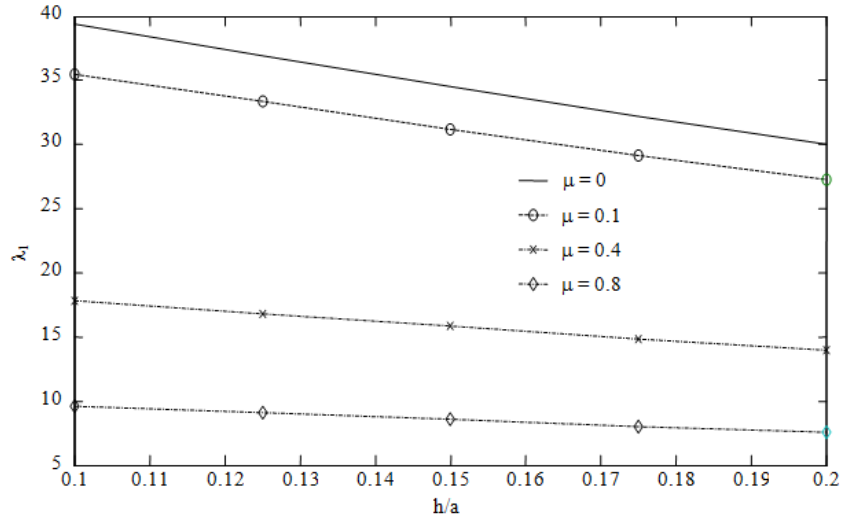


Fig. 7: Variation of the fundamental frequency parameter λ_1 with h/a of a CC non-local annular mindlin plate ($b/a = 0.3$)

Table 2: The first six frequency parameters of CC non-local annular mindlin plates with $b/a = 0.3$, $h/a = 0.15$

	μ								
	0	0.1	0.2	0.3	0.4	0.5	0.6	0.7	0.8
λ_1	34.5294	31.1961	24.9421	19.6324	15.8283	13.1349	11.1756	9.7029	8.5621
λ_2	77.7863	57.3769	37.1157	26.4060	20.2968	16.4284	13.7788	11.8567	10.4011
λ_3	128.7380	77.0506	45.2726	31.4442	23.9858	19.3547	16.2090	13.9364	12.2194
λ_4	182.9789	89.8115	49.7184	33.8884	25.6244	20.5788	17.1854	14.7493	12.9164
λ_5	239.3074	98.4831	52.9288	35.9042	27.1248	21.7814	18.1907	15.6134	13.6741
λ_6	294.4169	104.3338	54.8905	36.9886	27.8513	22.3228	18.6215	15.9713	13.9806

Table 3: The first six frequency parameters of CS non-local annular mindlin plates with $b/a = 0.3$, $h/a = 0.15$

	μ								
	0	0.1	0.2	0.3	0.4	0.5	0.6	0.7	0.8
λ_1	24.9426	22.6162	18.2231	14.4483	11.7090	9.7498	8.3141	7.2294	6.3862
λ_2	69.6681	51.8370	33.9405	24.3365	18.7913	15.2510	12.8129	11.0378	9.6900
λ_3	122.6923	73.4614	43.0503	29.7936	22.6684	18.2620	15.2781	13.1271	11.5044
λ_4	179.3020	87.7813	48.5780	33.1274	25.0618	20.1345	16.8187	14.4372	12.6447
λ_5	237.2397	97.1989	52.0769	35.2382	26.5781	21.3209	17.7947	15.2671	13.3670
λ_6	292.9046	103.5606	54.4192	36.6637	27.6081	22.1297	18.4617	15.8351	13.8619

Table 4: The first six frequency parameters of SS non-local annular mindlin plates with $b/a = 0.3$, $h/a = 0.15$

	μ								
	0	0.1	0.2	0.3	0.4	0.5	0.6	0.7	0.8
λ_1	19.2959	17.6440	14.4443	11.6016	9.4820	7.9377	6.7923	5.9198	5.2377
λ_2	63.6043	47.4485	31.0961	22.2728	17.1782	13.9302	11.6966	10.0721	8.8399
λ_3	118.4722	70.7583	41.3445	28.5486	21.6901	17.4584	14.5975	12.5376	10.9849
λ_4	176.9018	86.1921	47.5392	32.3506	24.4434	19.6228	16.3834	14.0591	12.3109
λ_5	236.2337	96.2536	51.4365	34.7523	26.1888	20.9977	17.5193	15.0275	13.1553
λ_6	289.0267	102.9765	54.0059	36.3431	27.3482	21.9125	18.2758	15.6730	13.7184

Table 5: The first six frequency parameters of clamped non-local circular mindlin plates

μ	h/a	Axisymmetric vibration mode number					
		1	2	3	4	5	6
0	0.100	9.9408	36.4787	75.6643	123.3195	176.4146	232.9659
	0.150	9.6286	33.3934	65.5507	102.0891	140.9321	180.9852
	0.200	9.2400	30.2107	56.6823	85.5714	115.5549	145.9428
0.1	0.100	9.6161	31.6709	56.8423	79.5243	98.1943	113.0861
	0.150	9.3175	29.0687	49.4716	66.1621	78.7687	88.1076
	0.200	8.9454	26.3648	42.9225	55.6057	64.6894	71.1295
0.2	0.100	8.8012	24.0185	37.4530	48.0005	56.1329	62.4317
	0.150	8.5347	22.1136	32.6962	40.0212	45.0845	48.6706
	0.200	8.2019	20.1216	28.4416	33.6805	37.0390	39.2838
0.4	0.100	6.8390	14.6684	20.8132	25.5858	29.2861	32.1744
	0.150	6.6408	13.5292	18.1877	21.3444	23.5289	25.0864
	0.200	6.3927	12.3364	15.8383	17.9713	19.3325	20.2467
0.8	0.100	4.2412	7.8724	10.7674	13.0494	14.8344	16.2348
	0.150	4.1212	7.2617	9.4093	10.8862	11.9185	12.6586
	0.200	3.9711	6.6231	8.1950	9.1666	9.7934	10.2167

Table 6: The first six frequency parameters of simply supported non-local circular mindlin plates

μ	h/a	Axisymmetric vibration mode number					
		1	2	3	4	5	6
0	0.100	8.8679	36.0407	76.6756	126.2742	181.4644	239.9853
	0.150	8.7095	33.6744	67.8274	106.3971	146.8346	187.7949
	0.200	8.5051	31.1106	59.6450	90.0593	120.5651	149.6279
0.1	0.100	8.6374	31.3010	57.1736	80.2976	99.1666	114.1166
	0.150	8.4795	29.1904	50.4298	67.4625	80.0975	89.3279
	0.200	8.2761	26.9207	44.2729	57.1080	66.0530	72.2725
0.2	0.100	8.0378	23.7620	37.4886	48.1594	56.3460	62.6573
	0.150	7.8826	22.0964	32.9646	40.3503	45.4114	48.9630
	0.200	7.6833	20.3203	28.8658	34.0895	37.3955	39.5743
0.4	0.100	6.4725	14.5454	20.7957	25.5910	29.3254	32.2066
	0.150	6.3322	13.4761	18.2360	21.3943	23.5980	25.1394
	0.200	6.1531	12.3466	15.9289	18.0449	19.4107	20.3046
0.8	0.100	4.1569	7.8343	10.7683	13.0384	14.8484	16.2320
	0.150	4.0560	7.2355	9.4265	10.8846	11.9374	12.6620
	0.200	3.9276	6.6086	8.2204	9.1713	9.8121	10.2230

seen that as the frequency decreases as the ratio h/a increases (Han and Liew, 1999) and the decrease rate is higher at smaller values of the non-local scale effect. The variations of the first six frequency parameters with the non-local parameter for CC, CS and SS non-local annular Mindlin plates at $b/a = 0.3$, $h/a = 0.15$ are presented in Table 2 to 4. As in the annular plates, it is seen that as the non-local scale parameter increases, the frequency parameters decrease and this effect is more significant for higher modes. Moreover, it is observed that the frequency parameters are more affected by the nonlocal parameter when the annular plate has clamped boundary conditions as the structure becomes stiffer and more rigid. Additionally, at higher values of the non-local parameter, the frequency parameters get closer to each other and it is expected that the frequency parameters will no longer increase as the mode number increases at values of μ greater than 1.0.

The variations of the first six frequency parameters with the non-local parameter for clamped and simply supported non-local circular Mindlin plates with different values of the thickness to radius ratio h/a are presented in Table 5 and 6, respectively. It is observed that as the ratio h/a and the non-local parameter μ increase, the frequency parameters decrease. As in the

non-local annular plates, the frequency parameters are more effected by the nonlocal parameter when the circular plate has clamped boundary conditions and at higher values of the non-local parameter, the frequency parameters get closer to each other.

CONCLUSION

The free vibration analysis of non-local annular and circular Mindlin plates was investigated and the nonlocal elasticity theory is employed to derive the governing equations of motion, where the Chebyshev spectral collocation method was utilized to solve for the frequency parameters. Convergence analysis was carried out to determine the sufficient number of grid points to be used in the computations. The effects of the nonlocal scale parameter, the inner to outer radius ratio (for annular plates), the thickness to the outer radius ratio and the boundary conditions on the frequency parameters are examined. It was found that the nonlocal scale parameter has a significant effect especially for higher frequency modes. Therefore, the scale parameter should be taken into account when modeling micro/nano annular and circular plates. Moreover, it was observed that the effect of nonlocal parameter on

the frequencies of plates with clamped boundary conditions is more than that on plates with simply supported edges. In addition, it was found that the frequencies get closer to each other at higher values of the nonlocal scale parameter. The results presented herein may be useful for scientists working on and designing micro/nano annular and circular plates. For future work, it is suggested to study the free vibration analysis of nonlocal annular and circular Mindlin plates resting on elastic foundation, due to the fact that graphene sheets and circular nanotubes are found embedded in elastic medium, which will make the study more realistic as it has an industrial application.

ACKNOWLEDGMENT

Author acknowledges the support of King Faisal University.

REFERENCES

- Ansari, R., S. Sahmani and B. Arash, 2010. Nonlocal plate model for free vibrations of single-layered graphene sheets. *Phys. Lett. A*, 375: 53-62.
- Duan, W.H. and C.M. Wang, 2007. Exact solutions for axisymmetric bending of micro/nanoscale circular plates based on nonlocal plate theory. *Nanotechnology*, 18: 385704.
- Eringen, A.C., 1983. On differential equations of nonlocal elasticity and solutions of screw dislocation and surface waves. *J. Appl. Phys.*, 54: 4703-4710.
- Gürses, M., B. Akgöz and Ö. Civalek, 2012. Mathematical modeling of vibration problem of nano-sized annular sector plates using the nonlocal continuum theory via eight-node discrete singular convolution transformation. *Appl. Math. Comput.*, 219: 3226-3240.
- Han, J.B. and K.M. Liew, 1999. Axisymmetric free vibration of thick annular plates. *Int. J. Mech. Sci.*, 41: 1189-1109.
- Hashemi, S.H., M. Zare and R. Nazemnezhad, 2013a. An exact analytical approach for free vibration of Mindlin rectangular nano-plates via nonlocal elasticity. *Compos. Struct.*, 100: 290-299.
- Hashemi, S.H., M. Bedroud and R. Nazemnezhad, 2013b. An exact analytical solution for free vibration of functionally graded circular/ annular Mindlin nanoplates via nonlocal elasticity. *Compos. Struct.*, 103: 108-118.
- Lu, P., H.P. Lee, C. Lu and P.Q. Zhang, 2006. Dynamic properties of flexural b beams using a nonlocal elasticity model. *J. Appl. Phys.*, 99: 073510.
- Murmu, T. and S.C. Pradhan, 2009a. Vibration analysis of nano-single-layered graphene sheets embedded in elastic medium based on nonlocal elasticity theory. *J. Appl. Phys.*, 105: 064319.
- Murmu, T. and S.C. Pradhan, 2009b. Vibration analysis of nanoplates under uniaxial prestressed conditions via nonlocal elasticity. *J. Appl. Phys.*, 106: 104301.
- Murmu, T. and S. Adhikari, 2010a. Nonlocal transverse vibration of double-nanobeam systems. *J. Appl. Phys.*, 108: 083514.
- Murmu, T. and S. Adhikari, 2010b. Scale-dependent vibration analysis of prestressed carbon nanotubes undergoing rotation. *J. Appl. Phys.*, 108: 123507.
- Reddy, J.N., 2007. Nonlocal theories for bending, buckling and vibration of beams. *Int. J. Eng. Sci.*, 45: 288-307.
- Sari, M.S. and E.A. Butcher, 2011a. Free vibration analysis of rectangular and annular Mindlin plates with undamaged and damaged boundaries by the spectral collocation method. *J. Vib. Control*, 18: 1722-1736.
- Sari, M. and E.A. Butcher, 2011b. Three dimensional analysis of rectangular plates with undamaged and damaged boundaries by the spectral collocation method. *Proceedings of the 8th International Conference on Multibody Systems, Nonlinear Dynamics and Control (ASME IDETC'11)*, Washington, D.C., USA.
- Sari, M.S. and E.A. Butcher, 2012. Free vibration analysis of non-rotating and rotating Timoshenko beams with damaged boundaries using the Chebyshev collocation method. *Int. J. Mech. Sci.*, 60: 1-11.
- Sari, M., M. Nazari and E.A. Butcher, 2011. Effects of damaged boundaries on the free vibration of Kirchhoff plates: Comparison of perturbation and spectral collocation solutions. *J. Comput. Nonlin. Dyn.*, 7: 011011.
- Shakouri, A., T.Y. Ng and R.M. Lin, 2011. Nonlocal plate model for the free vibration analysis of nanoplates with different boundary conditions. *J. Comput. Theor. Nanos.*, 8: 2118-2128.
- Trefethen, L.N., 2000. *Spectral Methods in MATLAB*, Software, Environments and Tools. SIAM, Philadelphia.
- Wang, C.M., Y.Y. Zhang and X.Q. He, 2007. Vibration of nonlocal Timoshenko beams. *Nanotechnology*, 18: 105401.